

Future abrupt reductions in the Summer Arctic sea ice

Marika M Holland (1), Cecilia M Bitz (2) and Bruno Tremblay (3)

(1) National Center for Atmospheric Research
1850 Table Mesa Drive
Boulder, CO 80305 USA
Phone: 303-497-1734; Fax: 303-497-1700; Email: mholland@ucar.edu

(2) Atmospheric Sciences box 351640
University of Washington
Seattle WA 98195-1640 USA
Phone: 206-543-1339; Email: bitz@atmos.washington.edu

(3) Lamont Doherty Earth Observatory of Columbia University,
Palisades, NY 10964-8000 USA
Email: tremblay@ldeo.columbia.edu
Now at: McGill University
Department of Atmospheric and Oceanic Sciences
Montreal, Quebec Canada H3A 2K6

Abstract

We examine the trajectory of Arctic summer sea ice in seven projections from the Community Climate System Model and find that abrupt reductions are a common feature of these 21st century simulations. These events have decreasing September ice extent trends that are typically 4 times larger than comparable observed trends. One event exhibits a decrease from 6 million km² to 2 million km² in a decade, reaching near ice-free September conditions by 2040. In the simulations, ice retreat accelerates as thinning increases the open water formation efficiency for a given melt rate and the ice-albedo feedback increases shortwave absorption. The retreat is abrupt when ocean heat transport to the Arctic is rapidly increasing. Analysis from multiple climate models and three forcing scenarios indicates that abrupt reductions occur in simulations from over 50% of the models and suggests that reductions in future greenhouse gas emissions moderate the likelihood of these events.

1 **Introduction**

2 Arctic sea ice has undergone dramatic changes in recent years with considerable
3 thinning of the ice pack (Rothrock et al., 1999; Wadhams and Davis, 2000), a sharp
4 reduction in the multi-year ice area (Johannessen et al., 1999; Comiso, 2002), and record
5 minimum September ice cover (Serreze et al., 2003; Stroeve et al. 2005). These changes
6 have led to the suggestion that a “tipping point” may have been reached in which strong
7 positive feedbacks accelerate ice retreat and result in an era of thinner, less extensive ice
8 cover in the Arctic (Lindsay and Zhang, 2005). However, the patchy observational record
9 and considerable natural variability in the Arctic make it difficult to assess whether a
10 tipping point has actually been reached.

11 Evidence is mounting that the observed changes are associated with anthropogenically
12 driven climate change (Vinnikov et al., 1999; Johannessen et al., 2004) and climate
13 models predict Arctic change to continue into the foreseeable future (Houghton et al.,
14 2001; Arzel et al., 2005; Zhang and Walsh, 2006). The transition from perennial to
15 seasonal Arctic ice cover has numerous implications for the climate system. Additionally,
16 the rate and manner in which sea ice retreats affects the ability of ecosystems and
17 societies to adapt to these changes. Here we examine the potential for abrupt transitions
18 in the future Arctic summer sea ice from climate models that have contributed output to
19 the Intergovernmental Panel on Climate Change fourth assessment report (IPCC-AR4).

20 **Model Simulations**

21 We analyze seven ensemble members of 20th and 21st century simulations from the
22 Community Climate System Model, version 3 (CCSM3) (Collins et al., 2006a). The
23 atmospheric component uses the Community Atmosphere Model, version 3 (Collins et

24 al., 2006b) which uses T85 (~1.4 degree) resolution and 26 vertical levels. The ocean
25 component (Smith and Gent, 2004) uses an isopycnal transport parameterization (Gent
26 and McWilliams, 1990) and surface boundary layer vertical mixing from Large et al.
27 (1994). The model is run at a nominally 1-degree resolution with the north pole displaced
28 into Greenland. No filtering is used in the ocean model at high latitudes. The Community
29 Sea Ice Model (Briegleb et al, 2004; Holland et al., 2006) uses energy conserving
30 thermodynamics (Bitz and Lipscomb, 1999), an elastic-viscous-plastic rheology (Hunke
31 and Dukowicz, 1997), and a subgridscale ice thickness distribution (Thorndike et al.,
32 1975). It is run on the same grid as the ocean model and uses five ice thickness categories
33 plus an open water category. The land component (Bonan et al., 2002) includes a subgrid
34 mosaic of plant functional types and land cover types as derived from satellite
35 observations. It is run on the same grid as the atmosphere model.

36 The simulations discussed here were performed as a contribution to the IPCC-AR4.
37 They include integrations from 1870-1999 in which different ensemble members were
38 initialized from different Januaries of a multi-century “preindustrial” control run with
39 constant external forcings based on 1870 conditions. The 1870-1999 integration was
40 driven with variations in sulfates, solar input, volcanoes, ozone, a number of greenhouse
41 gases, halocarbons, and black carbon that are based on the observed record and offline
42 chemical transport models. The simulations were then continued through the 21st century
43 using the *Special Report on Emission Scenarios* (SRES) A1B forcing (Houghton et al.,
44 2001). This scenario reaches 720ppm CO₂ levels by 2100 and is one of the “middle of
45 the road” SRES scenarios used in IPCC runs.

46 Results from 15 additional models (Auxiliary Material) are also discussed. These

47 model simulations are available through the IPCC-AR4 archive maintained by the
48 Program for Climate Model Diagnosis and Intercomparison (PCMDI). All of these
49 models incorporate a dynamic-thermodynamic sea ice model but they differ in their
50 resolution, component physics and physical parameterizations. They also differ in their
51 simulated polar climate (Arzel et al., 2006; Zhang and Walsh, 2006). Model simulations
52 using the SRES B1 forcing, which reaches 550 ppm CO₂ by 2100, and the SRES A2
53 forcing, which reaches 850 ppm CO₂ by 2100, are also discussed.

54 **CCSM3 Results**

55 The CCSM3 simulations compare well to the observed ice cover including the rate of
56 its recent retreat (Fig 1a; Holland et al., in press). The simulations do not however
57 indicate that ice retreat will continue at a constant rate into the future. Instead, they show
58 abrupt transitions that suggest near ice-free Septembers could be reached within 30-50
59 years. The simulated changes are surprisingly rapid. To illustrate these changes and the
60 mechanisms driving them, we present the results from one realization (Run 1) of a group
61 of seven ensemble members. To demonstrate the robustness of the results, we evaluate
62 other ensemble members of the same model and simulations from other models.

63 In the 20th century, the rate of the simulated September ice retreat is in accord with
64 observations (Fig. 1a). From 1979-2005, the Run 1 ice extent decreases by 10% per
65 decade, which is consistent with the observed 8% per decade decrease when accounting
66 for intrinsic variability as assessed from the different ensemble members. The late-20th
67 century Arctic is mostly covered with perennial ice, with reduced concentration in
68 summer along the shelves where first year ice melts away (Fig. 1b). The simulated ice
69 declines rapidly from 1998 to 2003, losing 20% of its extent in 6 years. The rate of

70 change then becomes more modest again until 2024. From 2003-2024, the simulated
71 Arctic (Fig. 1b) still has more than 60% perennial coverage, although, compared to the
72 late 20th century, the September ice concentration is reduced with large open water areas
73 along the Arctic shelves. Starting in 2024, the September ice retreats rapidly from
74 approximately 6 million km² to 2 million km² in a decade (Fig. 1). Over this event, the
75 trend of the 5-year running mean smoothed timeseries is -0.4 million km² per year, which
76 is over 3 times larger than any comparable trend in any 10-year interval of the observed
77 1979-2005 record (Fetterer and Knowles, 2002) and about 5 times larger than any
78 comparable 10-year trend of the simulated 20th century timeseries. After this event, by
79 2040, a small amount of perennial ice remains along the north coast of Greenland and
80 Canada, leaving the majority of the Arctic basin ice free in September (Fig. 1b).

81 There are multiple factors that contribute to this simulated abrupt change in September
82 ice cover. The globe warms over the 21st century and reductions in annual average ice
83 extent exhibit a nearly linear relationship with the global warming after approximately
84 2020. This is similar to previous modeling studies (Gregory et al., 2002). However,
85 summer ice cover reductions are not linearly related to the global-averaged air
86 temperature but instead exhibit the signature of the abrupt retreat.

87 An analysis separating the contributions to the ice extent change from thermodynamics
88 and dynamics indicates that the abrupt change is thermodynamically driven, with ice
89 dynamic effects (i.e. transport or ridging) playing little direct role. Over the run (Fig. 2a),
90 the ice cover thins from about 4 m to less than 1 m. The abrupt transition in September
91 extent is associated with large reductions in ice thickness, but these are similar to earlier
92 decreases that have little associated ice extent change (for example from 1920-1940). As

93 the ice pack thins, a given melt rate has a more direct influence on the summer minimum
94 ice extent, as large regions of ice can melt away completely, accelerating open water
95 formation. As such, “the efficiency of open water production” (defined as the percent
96 open water formation per cm of ice melt over the melt season) (Fig. 2b) increases
97 nonlinearly as the ice thins.

98 The relationship between thickness and rate of open water formation suggests that
99 there may be a critical winter ice thickness that is equal to the total potential for summer
100 melt. Once the threshold is reached, large regions of the ice pack could melt away. While
101 this is a reasonable idea, the reality of the model simulations is considerably more
102 complex. Analysis of the seven ensemble members lends no evidence that a common
103 critical state in the mean or distribution of ice thickness exists either regionally or at the
104 basin-scale. Instead, the interplay of simulated natural variability and forced change
105 influences the rate of summer ice retreat, contaminating any easily identifiable critical ice
106 state and making the prediction of the abrupt transitions difficult.

107 The increase in “open water production efficiency” with thinning hastens ice retreat
108 regardless of whether summer melt is increasing. However, basal melting clearly does
109 increase in part due to the surface albedo feedback, in which solar absorption in open
110 water increases as the ice retreats (Fig 3a). Over the melt season, this increased heating
111 warms the ocean mixed layer, increases basal melting, and delays the onset of ice growth.

112 Changes in ocean heat transport to the Arctic also play an important role in increasing
113 the net melt rate. Over the 20th and 21st centuries, this heat transport exhibits a gradual
114 upward trend overlaid by periods of rapid increase (Fig. 3a). These rapid “pulse-like”
115 events lead changes in the sea ice by 1-2 years, which is evident from the timeseries of

116 detrended heat transport and detrended ice thickness (Fig 3b). For Run 1, a rapid increase
117 in heat transport starts around year 2020, modifies the ice growth/melt rates, and triggers
118 positive feedbacks that then accelerate the ice retreat.

119 Increasing ocean heat transport to the Arctic occurs even while the North Atlantic
120 receives less poleward heat transport with a weakening meridional overturning
121 circulation. These increases are related to strengthened ocean currents and warmer waters
122 entering the Arctic Ocean from southern latitudes. Previous studies (Bitz et al., 2006)
123 suggest that such increases in future climate projections are associated with the changing
124 ice cover. As the ice cover thins, it becomes a weaker insulator resulting in larger ice
125 production during the autumn/winter. The consequent increase in winter brine rejection
126 drives ocean ventilation, and strengthens the inflow of warm Atlantic waters.

127 The simulated changes in ocean heat transport to the Arctic result in changes in
128 Atlantic layer heat content that are comparable to those in the observed record (Polyakov
129 et al., 2004). Many aspects of these changes have intriguing similarities to observations.
130 A warming of the intermediate depth Atlantic layer within the Arctic Ocean is observed
131 over the 20th century (Polyakov et al., 2004) with a gradual warming superimposed by
132 rapid, “pulse-like” events that originate in the Atlantic (Quadfasel et al., 1991; Polyakov
133 et al., 2005). Increases in the transport and temperature of the waters entering the Arctic
134 from the Atlantic are implicated in these warmings (Schauer et al., 2004; McLaughlin et
135 al., 1996; Swift et al., 1997), much like the model results.

136 **Results from other CCSM3 ensemble members**

137 How extraordinary is the abrupt transition in the September ice cover of the single
138 realization shown above? How robust are the processes that contribute to this transition?

139 Here we describe six additional ensemble members from the same model and the same
140 SRES A1B external forcing scenario. We identify an abrupt event when the derivative of
141 the five-year running mean smoothed September ice extent timeseries exceeds a loss of
142 0.5 million km² per year, equivalent to a loss of 7% of the 2000 ensemble mean ice extent
143 in a single year. The event length is determined by the time around the transition for
144 which the derivative of the smoothed timeseries exceeds a loss of 0.15 million km² per
145 year. While this definition is subjective, it clearly identifies rapid decreases in the ice
146 cover. Using these definitions, all of the ensemble members have rapid transitions in the
147 September ice cover (Fig. 4). The events generally last for 5 years and the rates of decay
148 over the events are about four times faster than a typical 5-year trend in the 1979-2005
149 smoothed observational timeseries or the simulated 20th century timeseries (Table 1). The
150 minimum trend over a simulated event is 2.7 times larger than any comparable trend in
151 any 5-year interval from the observations. The timeseries from Run 1 (Fig. 1a) is more
152 remarkable for the length of the abrupt change than for the rate of change. All of the
153 abrupt transitions are thermodynamically driven. All of the runs exhibit increased open
154 water production efficiency as the ice thins, increased solar radiation absorbed in the
155 ocean, and rapid increases in ocean heat transport to the arctic that lead and possibly
156 trigger the events.

157 **Results from other climate models**

158 Similar abrupt reductions in the September Arctic ice cover are present in a number of
159 future climate projections by other models participating in the IPCC-AR4 (Auxiliary
160 Material). In fact, six of an additional 15 models archived on the IPCC data center, also
161 exhibit abrupt September ice retreat in their A1B scenario runs. The length of the

162 transitions varies from 3 to 8 years among the models. Of the models that do not simulate
163 abrupt reductions, four have an unrealistic late 20th century ice extent and/or thickness.
164 This likely influences the possibility that abrupt transitions are simulated in the models.
165 Other aspects that may affect the simulation of abrupt events, including the intrinsic
166 variability in ice thickness and extent as assessed from the 20th century simulations and
167 differing sea ice model physics and resolution, have also been considered but no clear
168 relationship between these properties and the presence or absence of abrupt transitions
169 has been identified. Instead, multiple factors including the simulated climatology,
170 strength of feedback mechanisms, and modeled intrinsic variability play a complex and
171 interacting role in the future sea ice trajectory from the models.

172 The future emissions scenario used to force the model affects the likelihood of abrupt
173 sea ice reductions. In models forced with anthropogenic greenhouse gas levels increasing
174 at a slower rate (the SRES B1 scenario), only three of 15 models obtain abrupt transitions
175 lasting from 3-5 years. In simulations with anthropogenic greenhouse gas levels
176 increasing at a faster rate (the SRES A2 scenario), seven of 11 models with available data
177 obtain an abrupt retreat in the ice cover. The abrupt events in these runs last from 3-10
178 years and typically have larger rates of change.

179 **Concluding Remarks**

180 The possibility of abrupt transitions in the future Arctic sea ice has consequences for
181 the entire Arctic system. Here we have shown that CCSM3 climate model projections
182 suggest that abrupt changes in the summer Arctic sea ice cover are quite likely and can
183 occur early in the 21st century, with the earliest event in approximately 2015. These
184 transitions are associated with an increased open water formation efficiency for a given

185 melt rate as the ice thins. The surface albedo feedback accelerates the ice retreat as more
186 solar radiation is absorbed in the surface ocean, increasing ice melt. Additionally, rapid
187 increases in ocean heat transport to the Arctic generally lead and possibly trigger the
188 events.

189 An analysis of additional climate models and future forcing scenarios indicates that
190 abrupt transitions in the Arctic summer ice cover are not only present in the CCSM3
191 model but occur in numerous other projections of the future Arctic sea ice. Reductions in
192 future greenhouse gas emissions reduce the likelihood and severity of such events. A
193 recent study (Winton, submitted) also indicates that under higher emissions scenarios
194 some climate models exhibit abrupt transitions to completely ice-free conditions as first
195 year ice is also lost. Abrupt transitions such as those exhibited by climate models would
196 undoubtedly further strain adaptation of ecosystems and native peoples to climate change.

197

198 Acknowledgments: We acknowledge the international modeling groups for providing
199 their data for analysis, the Program for Climate Model Diagnosis and Intercomparison
200 (PCMDI) for collecting and archiving the model data, the JSC/CLIVAR Working Group
201 on Coupled Modeling (WGCM) and their Coupled Model Intercomparison Project
202 (CMIP) and Climate Simulation Panel for organizing the model data analysis activity,
203 and the IPCC Wg1 TSU for technical support. The IPCC Data Archive at Lawrence
204 Livermore National Laboratory is supported by the Office of Science, U.S. Department
205 of Energy. We thank two anonymous reviewers for helpful suggestions and thank NSF-
206 OPP and NSF-ATM for support.

References

- Arzel, O., T. Fichefet, and H. Goosse (2006), Sea ice evolution over the 20th and 21st centuries as simulated by current AOGCMs. *Ocean Modelling*, **12**, 401-415.
- Bitz, C.M., P.R. Gent, R.A. Woodgate, M.M. Holland, and R. Lindsay (2006), The influence of sea ice on ocean heat uptake in response to increasing CO₂. *J. Clim.*, **19**, 2437-2450.
- Bitz, C.M. and W.H. Lipscomb (1999), An energy-conserving thermodynamic model of sea ice. *J. Geophys. Res.*, **104**, 15,669-15,677.
- Bonan, G.B. et al. (2002), The land surface climatology of the Community Land Model coupled to the NCAR Community Climate Model, *J. Clim.*, **15**, 3123.
- Briegleb, B.P., C.M. Bitz, E.C. Hunke, W.H. Lipscomb, M.M. Holland, J.L Schramm, and R.E. Moritz (2004), Scientific description of the sea ice component in the Community Climate System Model, Version Three. NCAR Tech. Note. NCAAR/TN-463+STR.
- Collins, W.D. et al. (2006a), The Community Climate System Model: CCSM3, *J. Clim.*, **19**, 2122-2143.
- Collins, W.D., et al. (2006b), The formulation and atmospheric simulation of the Community Atmospheric Model: CAM3, *J. Clim.*, **19**, 2144-2161.
- Comiso, J.C. (2002), A rapidly declining perennial sea ice cover in the Arctic. *Geophys. Res. Lett.*, **29**, 1956, doi:10.1029/2002GL015650.
- Fetterer, F. and K. Knowles (2002), Sea ice index. National Snow and Ice Data Center, Digital Media, Boulder, CO., (updated).

- Gent, P.R. and J.C. McWilliams (1990), Isopycnal mixing in ocean circulation models, *J. Phys. Oceanogr.*, **20**, 150-155.
- Gregory, J.M., P.A. Stott, D.J. Cresswell, N.A. Rayner, C. Gordon, and D.M.H. Sexton (2002), Recent and future changes in Arctic sea ice simulated by the HadCM3 AOGCM, *Geophys. Res. Lett.*, **29**, doi:10.1029/2001GL014575.
- Holland, M.M., C.M. Bitz, E.C. Hunke, W.H. Lipscomb, and J.L. Schramm (2006), Influence of the sea ice thickness distribution on Polar Climate in CCSM3, *J. Clim.*, **19**, 2398-2414.
- Holland, M.M., J. Finnis, and M.C. Serreze (2006, in press), Simulated Arctic Ocean freshwater budgets in the 20th and 21st centuries, *J. Clim.*, in press.
- Houghton, J.T. *et al.*, Eds. (2001), *Climate Change 2001: The Scientific Basis*, Cambridge Univ. Press, Cambridge.
- Hunke, E.C. and J.K. Dukowicz (1997), An elastic-viscous-plastic model for sea ice dynamics, *J. Phys. Oceanogr.*, **27**, 1849-1867.
- Johannessen, O.M., E.V. Shalina, and M.W. Miles (1999), Satellite evidence for an Arctic sea ice cover in transformation, *Science*, **286**, 1937-1939.
- Large, W.G., J.C. McWilliams, and S.C. Doney (1994), Ocean vertical mixing: A review and a model with a nonlocal boundary layer parameterization, *Rev. Geophys.*, **32**, 363-403.
- Lindsay, R.W. and J. Zhang (2005), The thinning of Arctic sea ice, 1988-2003: Have we passed a tipping point? *J. Clim.*, **18**, 4879-4894.

McLaughlin, F.A., E.C. Carmack, R.W. Macdonald, and J.K.B. Bishop (1996), Physical and geochemical properties across the Atlantic/Pacific water mass front in the southern Canadian Basin, *J. Geophys. Res.*, **101**, 1183-1197.

Polyakov, I.V., G.V. Alekseev, L.A. Timokhov, U.S. Bhatt, R.L. Colony, H.L. Simmons, D. Walsh, J.E. Walsh, and V.F. Zakharov (2004), Variability of the intermediate Atlantic water of the Arctic Ocean over the last 100 years, *J. Clim.*, **17**, 4485-4497.

Polyakov, I.V. et al. (2005), One more step toward a warmer Arctic, *Geophys. Res. Lett.*, **32**, L17605, doi:10.1029/2005GL023740.

Quadfasel, D.A., A. Sy, D. Wells, and A. Tunik (1991), Warming in the Arctic, *Nature*, **350**, 385.

Rothrock, D.A., Y. Yu, and G.A. Maykut (1999), Thinning of the Arctic sea-ice cover, *Geophys. Res. Lett.*, **26**, 3469-3472.

Schauer, U., E. Fahrbach, S. Osterhus, and G. Rohardt (2004), Arctic warming through the Fram Strait: Oceanic heat transport from 3 years of measurements, *J. Geophys. Res.*, **109**, C06026, doi:10.1029/2003JC001823 .

Serreze, M.C. et al. (2003), A record minimum arctic sea ice extent and area in 2002, *Geophys. Res. Lett.*, **30**, 1110, doi:10.1029/2002GL016406.

Smith, R. and P. Gent (2004), Reference manual for the Parallel Ocean Program (POP) ocean component of the Community Climate System Model (CCSM2.0 and 3.0), LAUR-02-2484, Los Alamos National Laboratory, Los Alamos, New Mexico.

Stroeve, J.C., M.C. Serreze, F. Fetterer, T. Arbetter, W. Meier, J. Maslanik, and K. Knowles (2005), Tracking the Arctic's shrinking ice cover: Another extreme September minimum in 2004, *Geophys. Res. Lett.*, **32**, L04501, doi:10.1029/2004GL021810.

- Swift, J.H., E.P. Jones, K. Aagaard, E.C. Carmack, M. Hingston, R.W. MacDonald, F.A. McLaughlin, and R.G. Perkin (1997), Waters of the Makarov and Canada basins, *Deep Sea Res., Part I*, **48**, 1503-1529.
- Thorndike, A.S., D.S. Rothrock, G.A. Maykut, and R. Colony (1975), Thickness distribution of sea ice, *J. Geophys. Res.*, **80**, 4501-4513.
- Wadhams, P. and N.R. Davis (2000), Further evidence of ice thinning in the Arctic Ocean, *Geophys. Res. Lett.*, **27**, 3973-3975.
- Winton, M., Does the Arctic sea ice have a tipping point?, *Geophys. Res. Lett.*, submitted.
- Zhang, X. and J.E. Walsh (2006), Toward a seasonally ice-covered Arctic Ocean: Scenarios from the IPCC AR4 model simulations, *J. Clim.*, **19**, 1730-1747.

Figures

1. a) Northern Hemisphere September ice extent for Run 1 (black), the Run 1 five-year running mean (blue), and the observed five-year running mean (red). The range from the ensemble members is in dark grey. Light grey indicates the abrupt event. (b) The Run 1 (black) and observed (red) 1990s averaged September ice edge (50% concentration) and Run 1 conditions averaged over 2010-2019 (blue) and 2040-2049 (green). The Arctic region used in our analysis is shown in grey.

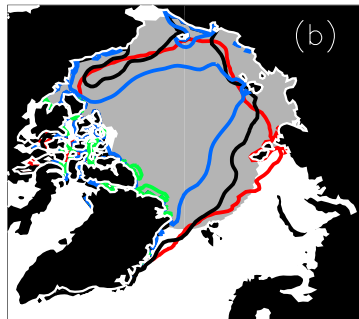
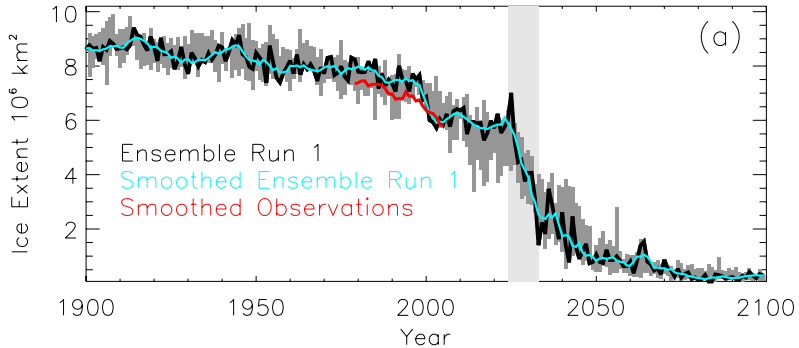
2. a) The Arctic averaged March ice thickness and b) the open water formation efficiency as a function of the March ice thickness for Run 1. The open water formation efficiency equals the open water formation (in percent) per cm of ice melt averaged over the melt season from May through August.

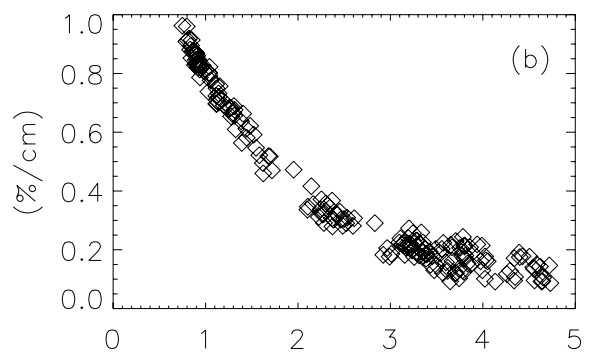
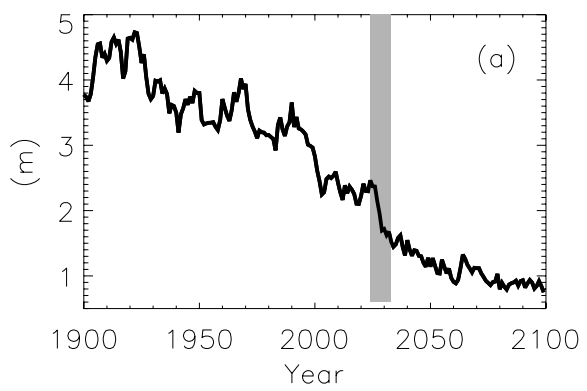
3. a) The anomalies relative to the 1990-1999 mean of Run 1 annual absorbed solar radiation in the Arctic Ocean (red) and ocean heat transport (OHT) to the Arctic (black). The OHT is integrated over the full ocean depth and includes transports through Fram Strait, the Barents Sea, the Bering Strait and the Canadian Archipelago. b) The 1950-2100 normalized and detrended negative OHT to the Arctic (black) and ice thickness (red). Thick lines show the five-year running mean. The abrupt event is shown in grey.

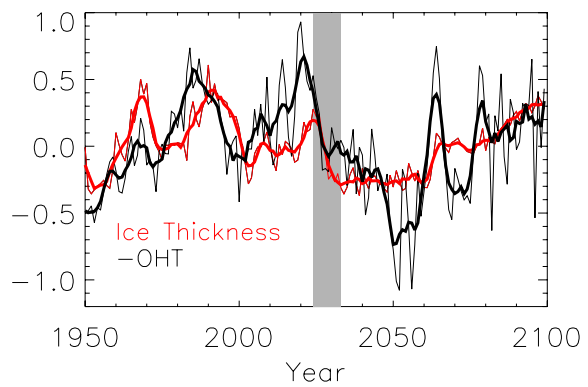
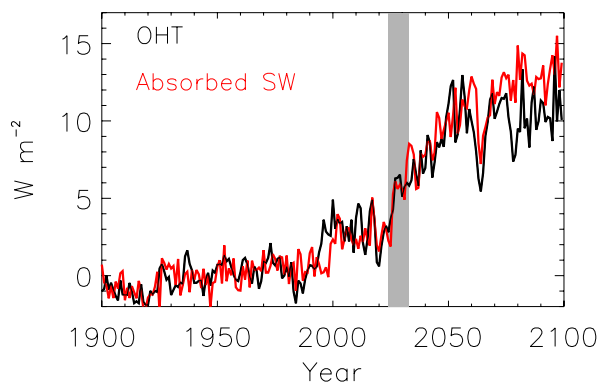
4. The Northern Hemisphere September ice extent from six additional CCSM3 A1B ensemble members. The five-year running mean (blue) and observed extent (red) are also shown. Grey shading indicates an abrupt transition as defined in the text.

Table 1. Information on the abrupt transitions in September ice extent from the CCSM3 ensemble members. The length is computed as defined in the text. The trend of the smoothed timeseries over the length of the abrupt event is shown in units of millions of square km per year.

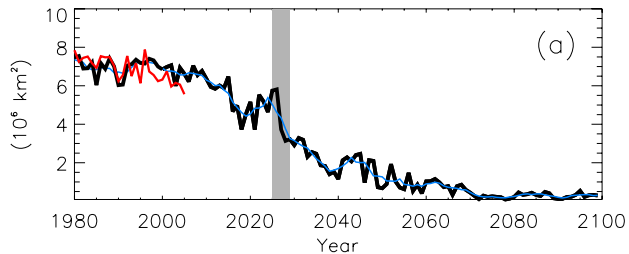
| Run | Years | Length (years) | Trend (10^6 km ² /year) |
|-------|-----------|----------------|---------------------------------------|
| Run 1 | 2024-2033 | 10 | -0.39 |
| Run2 | 2025-2029 | 5 | -0.44 |
| Run 3 | 2030-2034 | 5 | -0.42 |
| Run 4 | 2027-2034 | 8 | -0.32 |
| Run 5 | 2029-2034 | 6 | -0.51 |
| Run 5 | 2042-2045 | 4 | -0.41 |
| Run 6 | 2012-2016 | 5 | -0.49 |
| Run 6 | 2043-2047 | 5 | -0.38 |
| Run 7 | 2045-2049 | 5 | -0.39 |



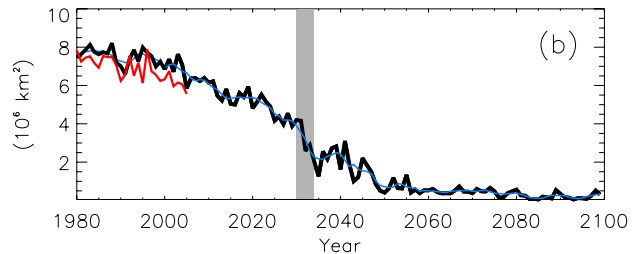




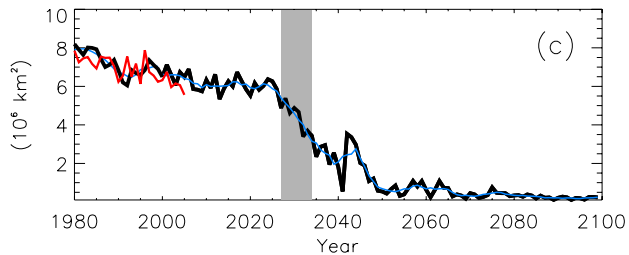
Run 2



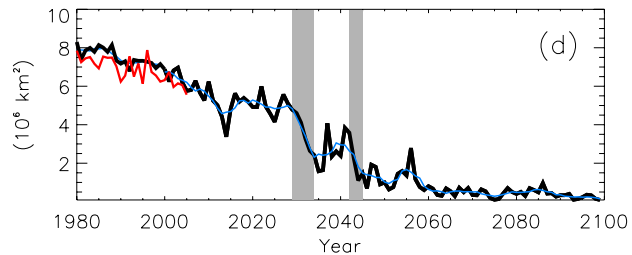
Run 3



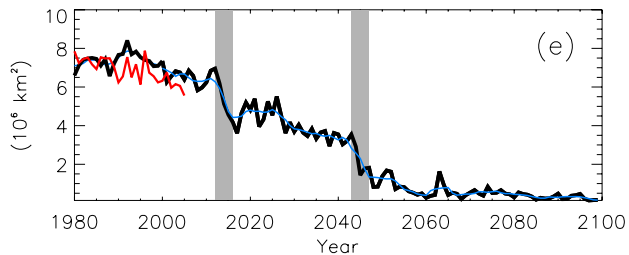
Run 4



Run 5



Run 6



Run 7

